Electron emission from carbon velvet due to incident xenon ions

M. I. Patino, and R. E. Wirz

Citation: Appl. Phys. Lett. **113**, 041603 (2018); doi: 10.1063/1.5037200
View online: https://doi.org/10.1063/1.5037200
View Table of Contents: http://aip.scitation.org/toc/apl/113/4
Published by the American Institute of Physics

Electron emission from carbon velvet due to incident xenon ions

M. I. Patino[a] and R. E. Wirz
Department of Mechanical and Aerospace Engineering, University of California, Los Angeles, California 90095, USA

(Received 22 April 2018; accepted 7 July 2018; published online 24 July 2018)

We present measurements of the ion-induced electron emission from carbon velvet. The results from carbon velvet with high aspect ratio vertical fibers (6.8 μm diameter and 2.6 mm length) show a more than 60% reduction in ion-induced electron emission for normal incident xenon ions over the entire ion incident energy investigated (i.e., 500–2000 eV) when compared to graphite. This is important for plasma-facing surfaces that are exposed to large fluxes of energetic ions, such as beam dumps and chamber walls used to control facility effects in plasma-thruster ground tests. *Published by AIP Publishing.* https://doi.org/10.1063/1.5037200

Electron emission from plasma-facing walls due to incident particles (i.e., electrons, ions, and fast neutral atoms) can lead to changes in plasma properties, including reduction in the sheath potential at the plasma edge, increased plasma electron energy loss to the walls, and cooling of the plasma bulk.[1] For example, materials with larger electron emission used in tokamaks[2,3] and Hall thrusters[4,5] were shown to produce plasmas with reduced sheath potential and electron temperature, respectively. Although electron-induced electron emission (commonly referred to as secondary electron emission, SEE) is typically much larger than ion-induced electron emission (IIEE), IIEE may be non-negligible, especially for low-Z incident ions.

Low energy incident ions may lead to the emission of electrons from the material via potential emission (i.e., Auger neutralization of ions at the surface) if the ionization potential of the incident ions is larger than twice the work function of the material.[6] At energies above a few keV, kinetic emission occurs whereby incident ions ionize and excite atoms within the material.[7] The generated electrons may release further electrons in electron-atom collisions as they diffuse to the surface. Only electrons with sufficient energy to overcome the retarding surface potential may be emitted.

Many recent experimental and modeling efforts have investigated textured materials to reduce SEE. These include metallic surfaces with nm to mm-sized vertical fibers/velvet,[5,8–15] isotropically aligned fibers/fuzz,[3,8,9,16] pores,[17,18] triangular and rectangular grooves,[19–21] soot particles,[22] and surface roughness.[23] For example, in a previous publication, we found that the SEE yield was reduced by more than 40% for tungsten fuzz generated in helium plasma under tokamak-like conditions when compared to smooth tungsten.[3] In contrast to SEE, there has been little previous work into IIEE from textured materials. IIEE has only been measured from tungsten fuzz for incident helium ions at 100 eV and was shown to be approximately 2× smaller than IIEE from smooth tungsten.[24]

This study explores the effect of material texturing on IIEE for a range of incident ion energies. IIEE is measured from carbon velvet due to incident xenon ions. Such carbon velvet materials have been used as beam dumps in in-lab testing of electric propulsion devices and may minimize the effect of electron emission from the vacuum chamber walls on the thruster electrical conduction pathway and in-lab performance.[25] Additionally, carbon velvet materials have been applied to the Hall thruster discharge channel,[11] utilized as a field emission cathode for high power microwave devices,[26] and proposed for the first wall in inertial confinement fusion devices.[27]

IIEE yields $\gamma = |I_{IIEE}|/I_I$ were measured in an ion beam facility (as described in Ref. 28) located at the Jet Propulsion Laboratory comprising three chambers: the source, filter, and test chambers. Xenon ions were created by a filament-cathode plasma source and accelerated to 500 eV or 1500 eV by a set of grids in the source chamber. Ions were focused and steered through two 3.2 mm diameter apertures located between the chambers, which are at 5° with respect to each other. This minimizes the amount of fast neutrals from the source chamber (e.g., created via charge-exchange) which reach the test chamber. Ions were then directed to a material sample mounted to the end of a cylindrical test cell (see Fig. 1) located in the test chamber. A collimator plate and front plate at the entrance to the test cell reduce the ion beam spot size to less than 10 mm, ensuring that ions impact the sample nearly normal to the surface. The background pressure within the test cell was measured by an ion gauge to be $\sim 5 \times 10^{-6}$ Torr. More details on the facility and test cell are found in Ref. 28.

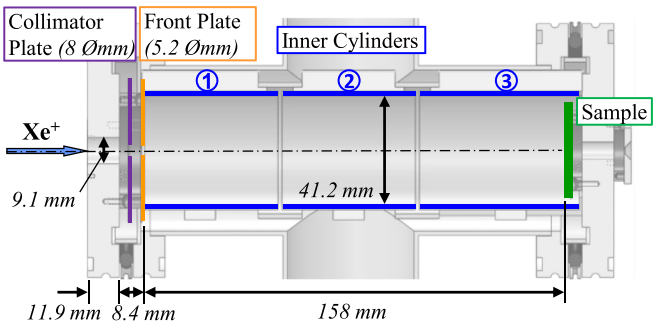

FIG. 1. Test Cell with sample and electron-collecting electrodes.

[a]Electronic mail: mipatino@ucla.edu

Incident ion energies between 500 eV and 2000 eV were achieved with a 500 eV or 1500 eV beam produced at the source by biasing the sample from −500 V to +500 V. Incident ion current was measured on the sample by biasing inner cylinders 2 and 3 to 50 V below the sample potential [i.e., $I_I = I_S(V_{IC23} = V_S - 50\text{V})$] to suppress electron emission. 500 eV and 1500 eV beams at the source resulted in ion currents of 2 nA and 30 nA, respectively, at the test cell (such small currents resulted in a space charge within the test cell of less than 0.01 V). Emitted electron current was measured on inner cylinders 2 and 3 and on the sample while inner cylinders 2 and 3 were biased to 50 V above the sample potential [i.e., $I_{IIEE} = I_{IC23}(V_{IC23} = V_S + 50\text{V})$ and $I_{IIEE} = I_S(V_{IC23} = V_I + 50\text{V}) - I_S$, respectively]. The front plate was kept at −50 V to prevent electrons created upstream of the test cell (e.g., from ions impinging on focus or deflection electrodes in the source and filter chambers) from entering the test cell. Similarly, the collimator plate was made from gold to avoid IIEE from this surface since gold has a low IIEE for incident xenon.[29,30] The inner cylinders were coated with nickel to prevent SEE from the electron collecting surfaces since nickel has a low SEE.[31] Keithley 236 and 237 source meters were used to apply voltage and read current from the sample, inner cylinders 2 and 3, and the front plate; Keithley 6485 picoammeters were used to read current from the remaining test cell electrodes. Error bars are calculated from Keithley instrumentation error, non-saturation of currents when suppressing/inciting IIEE, and reproducibility of measurements.

The carbon velvet sample [see Fig. 2(b)] was engineered by Energy Science Lab, Inc., and consisted of high-aspect ratio vertical fibers. The fiber diameter, length, and average packing density were 6.8 μm, 2.6 mm, and ∼80%, respectively, as determined with a Scanning Electron Microscope [SEM; see Fig. 2(c)]. No erosion of the fibers was observed with SEM after exposure to the low current density xenon ion beam. IIEE was also measured from a graphite sample [see Fig. 2(a)] for validation of the experimental setup and measurement approach. No pre-treatment of the carbon velvet or graphite samples was performed.

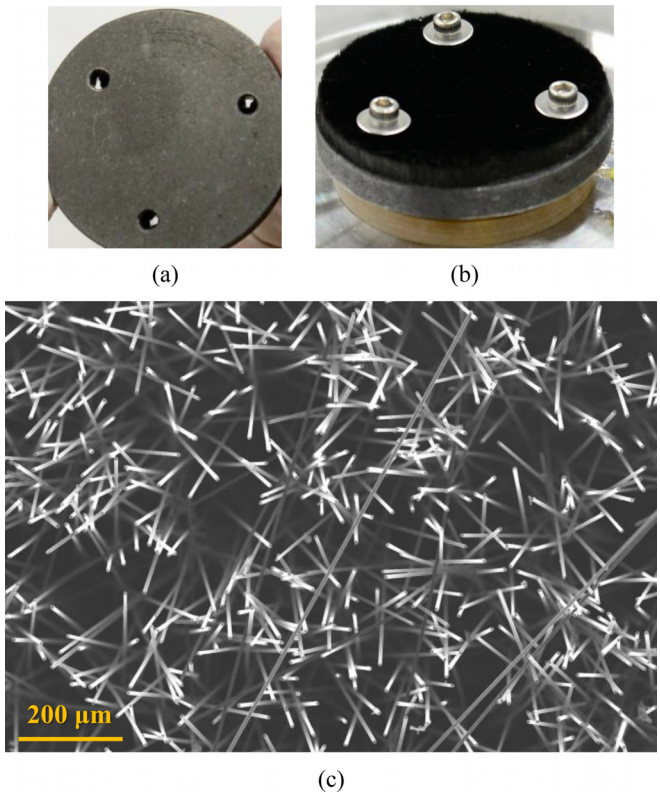

FIG. 2. (a) Graphite sample. (b) Carbon velvet sample. Note that during measurements of IIEE from carbon velvet, the carbon velvet was placed over graphite to facilitate mounting. (c) SEM image of carbon velvet (D_{fiber} = 6.8 μm, L_{fiber} = 2.6 mm, and packing density ∼80%).

Figure 3 shows the IIEE yield measured from graphite for xenon ions at normal incidence. The yield increases with incident ion energy, characteristic of kinetic electron emission. From theoretical calculations, the threshold for kinetic electron emission for xenon incident on graphite should occur at 1.3 keV.[7] However, Dennison *et al.*[32] observed a similar dependence of yield on energy for graphite at these low energies, and the yields compare well with our measurements. Deviation from this previous study is likely due to differences in grades of graphite (HOPG in Ref. 32 and Poco graphite in this work). It should be noted that there was good agreement between yields calculated from the sample and collector methods, and the yields plotted in Fig. 3 are the average of multiple measurements using both methods.

Also plotted in Fig. 3 is the IIEE yield from carbon velvet. Figure 3 shows a 60%–85% reduction in the IIEE from carbon velvet compared to "smooth" graphite. Similar reductions in the SEE yield have been observed for metallic surfaces with nm to mm-sized engineered and plasma-generated morphology, including fibers.[3,5,11–14] For example, Jin *et al.*[5] measured a 35% reduction in SEE (i.e., from a total SEE yield of ∼0.89 to 0.57) for carbon velvet with $D_{fiber} = 3$ mm, aspect ratio $A = 2L_{fiber}/D_{fiber} = 860$, and packing density = 87% due to electrons incident at 300 eV and 0°. Since the

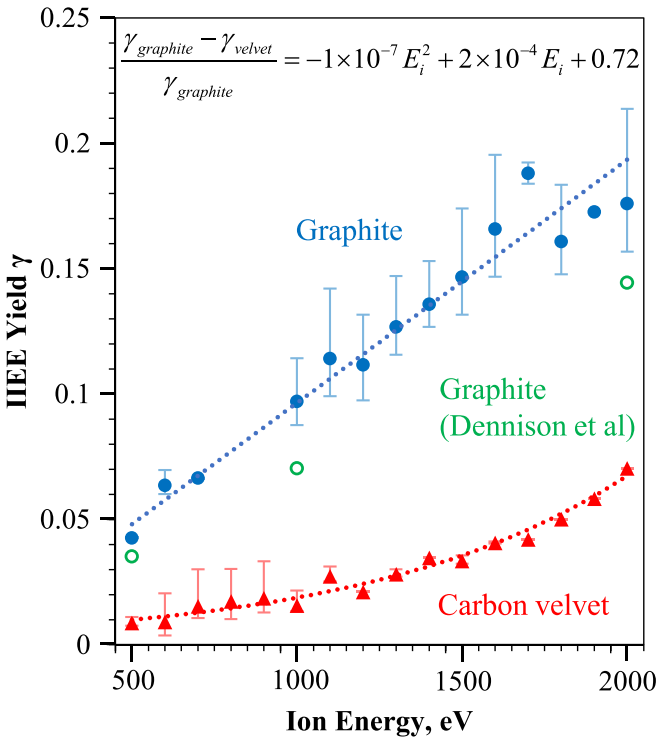

FIG. 3. IIEE yields from carbon velvet and graphite for xenon ions incident normal to the samples at 500–2000 eV. Measurements of graphite from Ref. 32 are plotted for comparison.

SEE yield is relatively flat above 200 eV,[3,5,9] it may be assumed that a nearly 35% reduction in SEE also occurs for 500 eV incident electrons. Analytical[10] and Monte Carlo[8–10,15,16] modeling of fibrous surfaces have confirmed that the reduction in SEE is due to trapping of emitted electrons (mostly true secondary electrons with a cosine angular distribution), especially for high aspect-ratio fibers.

Likewise, trapping of low energy emitted electrons generated by high energy ions is almost certainly responsible for the reduction in IIEE observed for carbon velvet in this work. For the carbon velvet considered herein, the fiber aspect ratio $A = 2L_{fiber}/D_{fiber} = 760$ and the packing density ~80%, very similar to the carbon velvet used by Jin *et al*. However, an 80% reduction was observed here for 500 eV xenon ions and only a 35% reduction from the study by Jin *et al*. for 500 eV electrons. The smaller reduction for incident electrons may be due to the fact that elastically and inelastically reflected primary electrons are considered by Jin *et al*. (in addition to true secondary electrons generated by ionization and excitation of atoms), and these reflected primary electrons are preferentially emitted from the material with angles near 0° for normal incidence. Thus, the reflected primary electrons are likely not effectively trapped but instead may escape the velvet material.

For materials with ordered vertical fibers such as carbon velvet, the SEE has been calculated[8–10] and measured[5] to increase with the incident angle. Since kinetic IIEE seems dominant at the energies considered herein and since kinetic IIEE occurs via a similar mechanism to SEE, an increase in IIEE with the ion incident angle may be expected for carbon velvet. The increase would be due to electron-generating collisions in the near-surface region along the walls of the fibers. Note that penetration depths of 2000 eV ions in carbon are on the order of a few nanometers. Therefore, negligible ions are able to transverse and re-emerge from a single fiber.

This work presents measurements of the IIEE from micro-engineered carbon velvet due to incident xenon ions at 500–2000 eV. Carbon velvet was found to reduce IIEE by 60%–85% when compared to graphite. The reduction in IIEE is larger than the reduction in SEE from a similar carbon velvet material. The substantial reduction in IIEE has important implications for many materials exposed to high energy ions. Although xenon ions were utilized in this study, similar reductions in IIEE are expected from textured surfaces for other incident ion species.

The authors would like to give their sincerest thanks to Lee Johnson of the Jet Propulsion Laboratory for much technical assistance with the ion beam facility, for many fruitful discussions on electron emission, and for providing the carbon velvet materials. This work was supported by AFOSR Award No. FA9550-14-10317 (UCLA Subaward No. 60796566-114411), the California Space Grant Consortium, and the UCLA Dissertation Year Fellowship.

[1]G. D. Hobbs and J. A. Wesson, Plasma Phys. **9**, 85 (1967).
[2]S. Takamura, T. Miyamoto, and N. Ohno, Plasma Fusion Res. **5**, 39 (2010).
[3]M. Patino, Y. Raitses, and R. Wirz, Appl. Phys. Lett. **109**, 201602 (2016).
[4]Y. Raitses, D. Staack, A. Dunaevsky, and N. J. Fisch, J. Appl. Phys. **99**, 036103 (2006).
[5]C. Jin, A. Ottaviano, and Y. Raitses, J. Appl. Phys. **122**, 173301 (2017).
[6]H. D. Hagstrum, Phys. Rev. **96**, 336–365 (1954).
[7]R. A. Baragiola, E. V. Alonso, J. Ferron, and A. Olivia-Florio, Surf. Sci. **90**, 240–255 (1979).
[8]C. E. Huerta and R. E. Wirz, AIAA Paper 2016-4840, 2016.
[9]C. E. Huerta, M. I. Patino, and R. E. Wirz, J. Phys. D: Appl. Phys. **51**, 145202 (2018).
[10]C. Swanson and I. D. Kaganovich, J. Appl. Phys. **120**, 213302 (2016).
[11]Y. Raitses, I. D. Kaganovich, and A. V. Sumant, in 33rd International Electric Propulsion Conference, Washington, DC, USA, 2013, Paper No. IEPC-2013-390.
[12]V. Baglin, J. Bojko, O. Grovner, B. Henrist, N. Hilleret, C. Scheuerlein, and M. Taborelli, in Proceedings of the 7th European Particle Accelerator Conference (EPAC 2000), Vienna, Austria, 2000.
[13]A. N. Curren, IEEE Trans. Electron Devices **33**, 1902 (1986).
[14]A. N. Curren, K. A. Jensen, and R. F. Roman, NASA Technical Paper No. 2967 (1990).
[15]C. Swanson and I. D. Kaganovich, J. Appl. Phys. **122**, 043301 (2017).
[16]C. Swanson and I. D. Kaganovich, J. Appl. Phys. **123**, 023302 (2018).
[17]M. Ye, Y. N. He, S. G. Hu, R. Wang, T. C. Hu, J. Yang, and W. Z. Cui, J. Appl. Phys. **113**, 074904 (2013).
[18]M. Ye, Y. N. He, S. G. Hu, J. Yang, R. Wang, T. C. Hu, W. B. Peng, and W. Z. Cui, J. Appl. Phys. **114**, 104905 (2013).
[19]A. A. Krasnov, Vacuum **73**, 195 (2004).
[20]M. Pivi, F. K. King, R. E. Kirby, T. O. Raubenheimer, G. Stupakov, and F. Le Pimpec, J. Appl. Phys. **104**, 104904 (2008).
[21]Y. Suetsugu, H. Fukuma, K. Shibata, M. Pivi, and L. Wang, in Proceedings of IPAC10 (2010), Paper No. TUPD043.
[22]H. Bruining, *Physics and Applications of Secondary Electron Emission* (McGraw-Hill, New York, 1954).
[23]N. Bundaleski, M. Belhaj, T. Gineste, and O. M. N. D. Teodoro, Vacuum **122**, 255 (2015).
[24]E. M. Hollmann, R. P. Doerner, D. Nishijima, and A. Yu. Pigarov, J. Phys. D: Appl. Phys. **50**, 445203 (2017).
[25]J. A. Walker, S. J. Langendorf, M. L. R. Walker, V. Khayms, D. King, and P. Pertson, J. Propul. Power **32**, 1365–1377 (2016).
[26]J. Yang, T. Shu, and Y. Fan, J. Appl. Phys. **113**, 043307 (2013).
[27]S. J. Zenobia, R. F. Radel, B. B. Cipiti, and G. L. Kulcinski, J. Nucl. Mater. **389**, 213–220 (2009).
[28]M. I. Patino and R. E. Wirz, Phys. Plasmas **25**, 062108 (2018).
[29]E. V. Alonso, M. A. Alurralde, and R. A. Baragiola, Surf. Sci. Lett. **166**, L155–L160 (1986).
[30]G. Lakits, F. Aumayr, M. Heim, and H. Winter, Phys. Rev. A **42**, 5780 (1990).
[31]R. L. Petry, Phys. Rev. **26**, 346 (1925).
[32]J. R. Dennison, C. D. Thomson, J. Kite, V. Zavyalov, and J. Corbridge, NASA Report No. 20040111058, 2004.